Uncovering Cortical Pathways of Prion-like Pathology Spreading in Alzheimer's Disease by Neural Optimal Mass Transport

Yanquan Huang[1,†], Tingting Dan[1,†], Won Hwa Kim[2], and Guorong Wu[1,3(✉)]

[1] Department of Psychiatry, University of North Carolina at Chapel Hill, Chapel Hill, NC 27599, USA
grwu@med.unc.edu

[2] Computer Science and Engineering/Graduate School of AI, POSTECH, Pohang 37673, South Korea

[3] Department of Computer Science, University of North Carolina at Chapel Hill, Chapel Hill, NC 27599, USA

Abstract. Tremendous efforts have been made to investigate stereotypical patterns of tau aggregates in Alzheimer's disease (AD), current positron emission tomography (PET) technology lacks the capability to quantify the dynamic spreading flows of tau propagation in disease progression, despite the fact that AD is characterized by the propagation of tau aggregates throughout the brain in a prion-like manner. We address this challenge by formulating the seek for latent cortical tau propagation pathways into a well-studied physics model of the optimal mass transport (OMT) problem, where the dynamic behavior of tau spreading across longitudinal tau-PET scans is constrained by the geometry of the brain cortex. In this context, we present a variational framework for dynamical system of tau propagation in the brain, where the spreading flow field is essentially a *Wasserstein* geodesic between two density distributions of spatial tau accumulation. Meanwhile, our variational framework provides a flexible approach to model the possible increase of tau aggregates and alleviate the issue of vanishing flows by introducing a total variation (TV) regularization on flow field. Following the spirit of physics-informed deep model, we derive the governing equation of the new TV-based unbalanced OMT model and customize an explainable generative adversarial network to (1) parameterize the population-level OMT using generator and (2) predict tau spreading flow for the unseen subject by the trained discriminator. We have evaluated the accuracy of our proposed model using the ADNI and OASIS datasets, focusing on its ability to herald future tau accumulation. Since our deep model follows the second law of thermodynamics, we further investigate the propagation mechanism of tau aggregates as AD advances. Compared to existing methodologies, our physics-informed approach delivers superior accuracy and interpretability, showcasing promising potential for uncovering novel neurobiological mechanisms.

[†] These authors contributed equally to this work.

Keywords: Tau propagation · Generative adversarial network · Graph neural network · Optimal mass transport · Alzheimer's disease.

1 Introduction

Tau, a protein associated with microtubules, serves as a critical regulator of microtubule stability and forms the primary constituent of neurofibrillary tangles, which are a principal neuropathological hallmark of Alzheimer's disease (AD) [9]. Following the seminal postmortem study in [3], tau pathology is often observed to initiate in the rostral medial temporal lobe, particularly in the entorhinal cortex at Braak stage I/II. Subsequently, it advances to limbic regions at Braak stage III/IV, encompassing the hippocampus. Ultimately, tau pathology extends to the neocortex at Braak stage V/VI, invariably correlating with cognitive symptoms [12], the propagation of tau is shown in Fig. 1 (left).

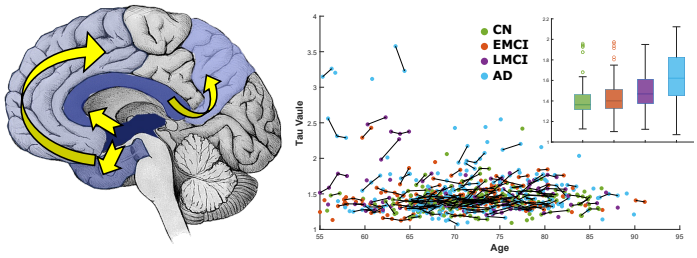

Fig. 1: Left: Propagation of tau pathology in AD. Right: Longitudinal change of whole-brain tau accumulation.

As is well known, the human brain is an intricately interconnected system formed by white matter fibers [1]. Within this framework, the concept of tau propagation emerges as a plausible mechanism through which tau pathology may systematically develop and advance across distinct brain regions [8]. A plethora of evidence suggests that abnormal tau aggregates do not appear randomly within the brain. Instead, their dissemination follows distinct spatial patterns, constrained by the cortical geometry [16, 21] and the intricate large-scale brain networks [11, 14, 15]. In this context, several graph diffusion models have been proposed to capture the temporal dynamics of tau propagation. For instance, the network diffusion model [14, 22] has been employed to forecast the future accumulation of pathological burdens, with spreading pathways delineated by the network topology. Current research on tau biomarkers predominantly focuses on the association between local accumulation of tau aggregates and disease severity. For example, cross-sectional examinations of tau pathology reveal a stereotypical pattern that varies between cognitive normal (CN), early-stage mild cognitive decline (EMCI), late-stage MCI (LMCI), and AD. However, subject-specific evolution of tau aggregates manifests inconsistent changes (indicated by lines within the same subject in Fig. 1 (right)) as the disease progresses, which poses a significant challenge to correlating longitudinal change with disease progression.

Prevailing computational models often simplify system linear dynamics as linear [15, 18], which may lead to inconsistent findings on tau propagation. For instance, commonly used techniques involve utilizing eigenvectors of the graph Laplacian matrix (derived from the brain network's adjacency matrix) as basis functions to model longitudinal changes in pathological burdens across brain regions. By assuming that future changes will adhere to the same dynamics, these methods project tau accumulations via extrapolation in the temporal domain. Nevertheless, these approaches predominantly capture focal changes at individual nodes, thus lacking the capacity to fully elucidate the mechanism driving tau propagation over time. Another critical limitation in current methods is focusing on only a few regions (i.e., the *region-to-region* spreading via bundles of white matter fibers) rather than voxel-based alterations, such as brain cortex.

Even though we can accurately predict the longitudinal changes of focal patterns at each node, multiple flow-spreading scenarios can lead to equivalent time-varying regional measurements. In contrast, understanding the emerging flow-spreading mechanism facilitates straightforward explanation and prediction of focal pattern trends. Therefore, uncovering the region-to-region (or vertex-to-vertex) flow map underlying tau propagation is valuable. Solving this reverse problem could discover new insights into the etiology of AD in neuroscience. Drawing an analogy to a public transportation system, we conceptualize that the macro-environment propagation of tau aggregates throughout the brain entails a primary mode of neural transportation, i.e., the prion-like *cell-to-cell* spreading along the brain cortex. By constraining tau spreading flows atop the brain cortex, we translate the tau-specific transport equation (similar to the optimal mass transport problem, OMT) into an equivalent graph neural network (GNN). This approach, executed in a layer-by-layer manner, enables effective characterization of tau spreading flows from a multitude of longitudinal tau-PET scans [7]. The network topology is constructed based on the spatial distances between vertices on the brain surface. Therefore, our proposed method represents an explainable deep model, with physics principles providing the system-level underpinning of tau spreading flows, while the mathematical insight and the power of deep learning ensure application value, such as prediction accuracy.

We have applied our proposed method to longitudinal neuroimaging data from the ADNI and OASIS datasets, enabling us to evaluate the prediction accuracy of future tau accumulation and explore the propagation mechanism of tau aggregates as the disease progresses. In addition, we investigate the trending of cortical thickness (CT) reduction on the cortex, where CT is regarded as an outcome proxy of pathological process.

2 Method

Consider the brain cortex is a collection of vertices $\mathcal{G} = (\nu, \varepsilon)$, where the set of vertices ($\nu = 1, ..., N$) forms the brain surface, and each vertex represents a node in the graph. The relationships between these vertices are captured using an adjacency matrix $D = [d_{ij}]_{i,j}^{N}$, the construction method of graph topology is

illustrated in Fig. 2 (c), i.e., $d_{ij} = \sqrt{(a_i - a_j)^2 + (b_i - b_j)^2 + (c_i - c_j)^2}$, where d_{ij} represents the Euclidean spatial distance between interconnected nodes i and j, and variables a, b, c denote the coordinates of vertex. For nodes without repeated edges or self-loops, related edges are set as 0. Each node ν_i is associated with feature embeddings x_i, which are the nodal measurements of tau SUVR (standard uptake value ratio) or cortical thickness. As explained next, we seek to forecast changes in biomarkers (such as tau or cortical thickness (CT)) in the brain by uncovering the latent vertex-to-vertex flow field between current and next time points.

2.1 GNNs with a Link-Selective Information Exchange Mechanism

GNNs [20] has emerged as a powerful framework for learning representations of graph-structured data. In GNNs, nodes in a graph are associated with feature vectors, and the relationships between nodes are encoded in the graph structure. GNNs optimize by iteratively aggregating feature x_i from neighboring nodes ν_i, allowing them to capture complex patterns and dependencies within the graph. During backpropagation, each node receives gradients as $\nabla_{\mathcal{G}} x = d_{ij}(x_i - x_j)$ at each layer of the GNN. Essentially, GNN captures the relationships between feature nodes by following a graph heat kernel process where the regularization can be formulated as $\mathcal{L}_{heat} = \int_{\mathcal{G}} |\nabla_{\mathcal{G}} x|^2 dx$. In an analogy to the isotropic Gaussian smoothing, this l_2-regularized optimization approach tends to overly smooth the final results. To mitigate this issue, the total variation (TV) regularization [6] is applied to the graph smoothness term. The TV-based graph regularization is then formulated as follows: $\mathcal{L}_{TV} = \int_{\mathcal{G}} |\nabla_{\mathcal{G}} x| dx$, which allows us to selectively exchange nodal information via following a global heuristics such as network community (i.e., applying graph heat kernel diffusion within the community while maintaining the community-to-community distinction).

2.2 Variational Framework of OMT Model for Tau Propagation

Problem formulation. We consider the tau accumulation at the baseline t and follow-up t+1 as the probability distribution ρ^t and ρ^{t+1} (by normalizing x across brain cortex). For a given probability function ρ and a vector field $v \in \mathcal{R}^{N \times N}$, $q = \rho v \in \mathcal{R}^{N \times N}$ is the *flux field* on $\mathcal{G}$. In this context of OMT, we seek to find a vector field v, which has the lowest cost to transport the mass of tau aggregate from ρ^t to ρ^{t+1}. If the transport cost between two brain regions is measured using l_2-norm distance, the specific infimum is called the *Wasserstein*-2 distance ($\mathcal{W}_2$). Benamou and Brenier theory [2], pointed out that *Wasserstein*-2 distance can be written in an equivalent computational fluid dynamic formulation which boils down to the Fokker-Plank (FP) equation [13].

$$\begin{aligned} \mathcal{W}_2\left(\rho^t, \rho^{t+1}\right) &= \inf_v \int_t^{t+1} \rho \|v\|^2 dt \\ \text{subject to:} \quad \frac{d\rho}{dt} + div(\rho v) &= 0, \quad \rho(t) = \rho^t, \quad \rho(t+1) = \rho^{t+1} \end{aligned} \tag{1}$$

where ρ is time-interpolant between ρ^t and ρ^{t+1} over time interval $[t \to t+1]$ and div denotes the divergence operator. Inspired by [7], we conceptualize the tau spreading dynamics as a conservative system of transporting the mass of tau aggregates where the spreading flow is optimized towards the minimal cost in terms of geodesic distances on brain cortex. Moreover, formulating tau propagation using OMT allows us to develop explainable deep models with great mathematical insight. To that end, we will use deep learning techniques to parameterize the transport maps that can be applied to incoming unseen subjects.

OMT equation for cortical Tau propagation. Upon the introduction in Sec. 2.1, we first replace $\mathcal{W}_2$ with *Wasserstein*-1 distance $\mathcal{W}_1\left(\rho^t, \rho^{t+1}\right) = \inf_v \int_t^{t+1} \rho|v|dt$, to prevent flow vanishing issue. The motivation of using $\mathcal{W}_1$ OMT is that (1) OMT with linear ground distance is usually more robust to outlier and noise than a quadratic cost, and (2) TV-based deep models are more effective at maintaining the data geometry compared to those based on l_2-norm [6]. Similar to the gravity field driving water flow, the intuition of OMT is that the evolution of latent potential function u (we assume there is a non-linear mapping ϕ from tau SUVR x to u, i.e., $u = \phi(x)$ steers the propagation of tau aggregates throughout the brain cortex. Further, we constrain the gradient of the potential function $\nabla_{\mathcal{G}} u$ to follow the graph topology $(\nabla_{\mathcal{G}} u)_{ij} = d_{ij}(u_i - u_j)$. Following the recent work [5, 7], we assume the energy flux q is regulated by the potential gradient field $\nabla_{\mathcal{G}} u$, i.e., $q = \alpha \otimes \nabla_{\mathcal{G}} u$, where $\alpha = [\alpha_{ij}]_{i,j=1}^N$ is a learnable matrix characterizing the link-wise contribution of each potential gradient $(\nabla_{\mathcal{G}} u)_{ij}$ to the flux q_{ij} and $\otimes$ denotes Hadamard production. Therefore, the physical concept of flow defined as $q = \rho v$ is equivalent to the machine learning counterpart $q = \alpha \otimes \nabla_{\mathcal{G}} u$. This prompts a reformulation of the *Wasserstein*-1 distance as

$$\mathcal{W}_1\left(\rho^t, \rho^{t+1}\right) = \inf_v \int_t^{t+1} \rho|v|dt \tag{2}$$

Since $\mathcal{W}_1$ is not differentiable at $u = 0$, we introduce a dual matrix variable $f \in \mathcal{R}^{N \times N}$ to approximate $|\nabla_{\mathcal{G}} u|$ with $f \cdot (\nabla_{\mathcal{G}} u)$ by expecting $|f| \to 1$, which boils down to the minimization of $\mathcal{W}_1$ to dual *min-max* functional

$$\mathcal{J}_{TV}(u, f) = \min_u \max_f \int_0^1 \alpha \otimes (f \cdot (\nabla_{\mathcal{G}} u))\, dt \tag{3}$$

After that, we use Gâteaux variations to optimize $\mathcal{J}_{TV}$ via the following two coupled time-dependent PDEs: $\begin{cases} \max_f \frac{df}{dt} = \alpha \otimes \nabla_{\mathcal{G}} u \\ \min_u \frac{du}{dt} = -\alpha \otimes \mathrm{div}(f) \end{cases}$. Since α is a latent variable and tau potential energy u is given, the maximization of f opts towards maximizing the tau spreading flow via α, under the condition that the spreading flow f satisfies $u_i(t+1) = u_i(t) + \sum_{j=1}^N f_{ij}$ at each brain vertex. Given the tau flow f, we can update the tau potential function u by solving the FP equation. Second, we extend the above FP equation to an unbalanced OMT scenario where we allow the volume change of tau aggregates over time. In this regard, we

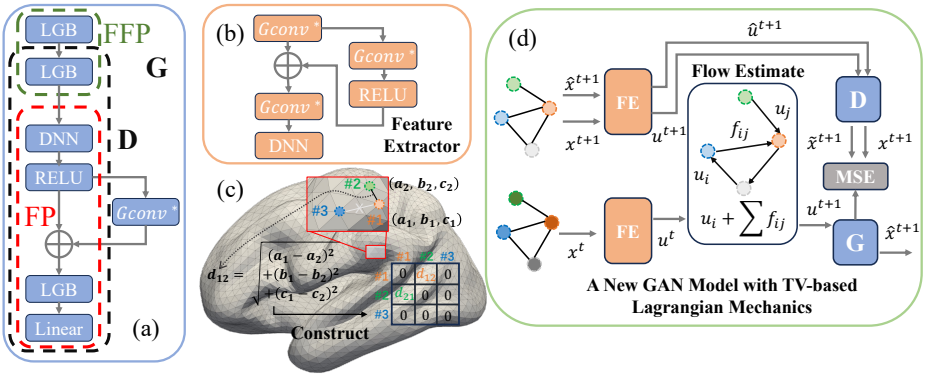

Fig. 2: (a) The network architecture of the generator (G) and discriminator (D). (b) the feature extractor (FE). (c) The construction of graph topology on the brain surface. (d) The framework of our proposed new GAN model with TV-based Lagrangian mechanics.

modify the FP equation to $\frac{du}{dt} + \alpha \otimes div(f) = \varphi(s)$, where s denotes the mass difference and φ is the reaction function. Thus, the change of potential u at each brain region is due to not only flux q in the graph neighborhood but also the production of new tau aggregates. Combining with PDE, we select GAN network architecture to implement the min-max optimization schema is that we sought to design an end-to-end deep model that allows us to include the learning component for capturing the reaction process (mapping from the observed tau concentration to the latent state) in brain cortex.

A GAN model of tau spreading flow with TV-based Lagrangian mechanics. By incorporating unbalanced OMT into tau prediction, we can better model the complex dynamics of tau propagation in the brain, taking into account the varying amounts of tau present in different cortex regions. This approach enhances the accuracy and robustness of our predictions, leading to more precise insights into neurodegenerative diseases and other neurological conditions associated with tau pathology. To optimize Eq. 3, we integrate unbalanced OMT to design a generative adversarial network (GAN) network model with TV-based Lagrangian mechanics to predict the spreading flow f. The overall network architecture is shown in Fig. 2 (d), mainly consisting of a generator (G) and discriminator (D) module (Fig. 2 (a)). To enable the network to acquire flow information, we reform the graph convolution (marked as Gconv*) operation as $\text{Gconv}^*(x_i) = \sum_{j=1}^{N} d_{ij} \cdot (W \cdot x_i)$, $\text{Gconv}^*(x)$ denotes the resulting feature vector after the Gconv* operation, N is the number of nodes, x_i represents the feature vector of the i-th vertex, W denotes the weight matrix for the linear transformation, $W(d_{ij})$ represents the weighting function based on the distance d_{ij}. This formula describes how the new Gconv* operation weights and sums the input features based on the distances between nodes, which are applied to GAN.

Specifically, x_t is fed into the feature extractor (FE) (Fig. 2 (b)) to yield latent potential function u^t, where FE is defined as: $F = \mathrm{RELU}(\mathrm{Gconv}^*(\mathrm{Gconv}^*(X)))$, $H = F + \mathrm{RELU}(\mathrm{Gconv}^*(F)), Y = \mathrm{DNN}(H)$, where $\mathrm{DNN}(\cdot)$ is composed of linear layers ($\phi(\cdot)$) and Leaky Relu activation functions, Y is the output of the final step of the features extractor. The proposed Gconv* component can optimize u_t through the unbalanced FP equation. u_t interacts with information from each interconnected node to generate u_{t+1}. Then fed into the generator and it can produce $\hat{x}^{t+1}$, which serves as input to the discriminator. The discriminator's process involves x^{t+1} passing through the feature extractor to generate energy density u^{t+1}. Information interaction is performed on u^t, which is then fed into the discriminator for decoding, yielding the final output $\tilde{x}^{t+1}$. The generator (G) (Fig. 2 (a)) is divided into a feature flow prediction module (FFP, green dashed box) and a feature prediction module (FP, red dashed box). The feature flow prediction module consists of two layers, with one layer dedicated to learning to update u through the equation $u_i(t+1) = u_i(t) + \sum_j^N f_{ij}$. After the feature flow prediction module, u^{t+1} can be obtained. In the feature decoding module, the decoding task is mainly performed by linear layer ($\phi(\cdot)$) and Gconv* block (short for LGB)) and DNN is crucial for decoding u^{t+1} back to the predicted future data $\hat{x}^{t+1}$. Note, since the working mechanism of this adversarial model underlines the *min-max* optimization in the energy transport equation, the nature of predicted spreading flows is carved by the characteristics of *max-flow*. The driving force of our network is to minimize (1) the mean square error (MSE) between the generator output $\hat{x}^{t+1}$ and observed tau SUVR x^{t+1} and (2) the distance between the synthesized $\tilde{x}^{t+1}$ (from discriminator) and the generator output $\hat{x}^{t+1}$.

3 Experiments

3.1 Data Description and Experimental Setting

We evaluate our model on ADNI [19] and OASIS [10] datasets. First, we selected 163 subjects from the ADNI dataset, each containing 2-5 time-series data points, therefore the amount of data has increased by 1.6 times. Especially, we use the standard MNI Space to register all the PET images and use the Gaussian function for denoising. Each individual had tau surface and cortical thickness data for both the left and right brain. All tau and cortical thickness data is presented by vertices of brain. The number of vertices is $N = 163842$ (decimating in *Freesurfer* can be used to reduce complexity). The involved cohorts are divided into four groups based on the diagnostic labels of each scan, including the CN group, EMCI group, LMCI group, and AD group. The data split strategy is 6:2:2 (training: validation: testing). To validate the generalization of our model, we select the OASIS dataset for predicting cortical thickness. OASIS dataset consists of 1172 subjects and the type of disease contains AD and CN.

The comparison method contains the prevail graph-based methods including vanilla GCN [20], GAT [17] and a current graph-based SOTA method GCNII [4] on predicting disease progression (i.e., future tau accumulation) on the ADNI

and OASIS datasets. The learning rate and epochs as (Generator: lr=0.001, Discriminator: lr=0.006 and Epoch: 30). The evaluation metrics for testing results including (1) mean absolute error (MAE) for predicting tau burden levels and (2) MAE for identifying predicted cortical thickness.

3.2 Results on Predicting Tau and Cortical Thickness

We perform a comprehensive series of experiments on both the ANDI and OASIS datasets to predict future tau burden based on baseline tau levels and cortical thickness. Table 1 (top) demonstrates the superior performance of our approach on forecasting further tau accumulation. To support the generalization of our model, we further assess its performance in predicting cortical thickness (bottom), a proxy measure that indirectly reflects disease progression. Our method also achieves considerable results. For OASIS dataset, our proposed method outperforms GCN, GCNII and GAT with MAE of 0.3621 compared to 0.3879, 0.8401 and 1.3457, respectively. As depicted in Fig. 3 (left), we examine the patterns of tau aggregate spread within both CN and AD groups. Notably, the highlighted regions in red denote significant areas characterized by heightened tau propagation. Particularly striking is the pronounced tau spreading observed in the temporal lobe during the advanced stages of AD, contrasted with the relatively subdued transport flow in CN subjects. In our visualization, color gradients represent varying levels of tau accumulation on the cortex, while the length of arrows corresponds to the volume of tau propagation flux. Fig. 3 (right) shows the reduction trend of CT (outcome proxy) on the cortex.

	Model	CN	AD	LMCI	EMCI	Mean
Tau	Ours	**0.2403**	**0.1318**	**0.2389**	**0.1865**	**0.2208**
	GCN	0.3951	0.1612	0.3286	0.2220	0.3277
	GCNII	0.6611	0.4631	0.6106	0.4729	0.6008
	GAT	1.2210	0.9633	1.1280	0.8761	1.1220
CT	Ours	**0.3107**	**0.3157**	**0.3143**	**0.3274**	**0.3145**
	GCN	0.3682	0.3619	0.3652	0.3721	0.3646
	GCNII	0.4637	0.4284	0.4493	0.4552	0.4429
	GAT	0.5960	0.5607	0.5693	0.5689	0.5716

Table 1: Performance comparison (Tau and Cortical Thickness) with different graph models on ANDI dataset.

4 Conclusion

In this work, we embarked on a variational framework for dynamical system of tau propagation in the brain, which is formulated as an OMT problem and customizes an explainable generative adversarial network. Experimental results show that our physics-informed method outperforms other GNN models, not only in predicting tau aggregation but also in cortical thickness, thereby enhancing our understanding of the pathophysiological mechanisms. However, our

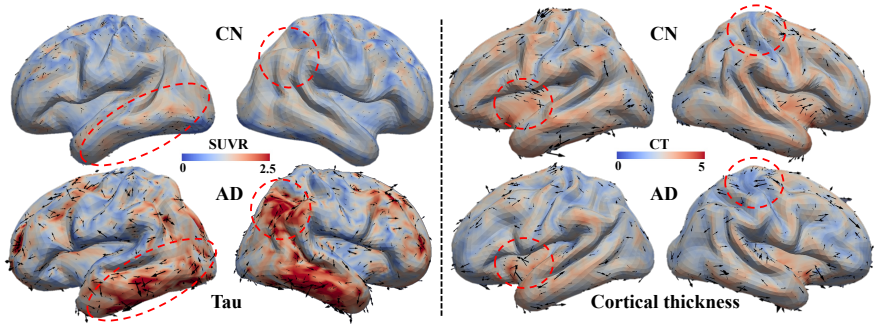

Fig. 3: Left: Cortical tau flows by OMT. We show the vertex-based cortical flows for one CN (top) and one AD (bottom) subject between two tau distributions on the brain cortex. Right: The decreasing trend of cortical thickness.

method has the limitation that predicting the tau and cortical thickness in specical time points.In future work, we may involve exploring innovative graph regularization techniques and conducting further precise predition based on specific time points of graph-based learning tasks.

Disclosure of Interests. The authors have no competing interests to declare.

References

1. Bassett, D.S., Sporns, O.: Network neuroscience. Nature neuroscience **20**(3), 353–364 (2017)
2. Benamou, J.D., Brenier, Y.: A computational fluid mechanics solution to the monge-kantorovich mass transfer problem. Numerische Mathematik **84**(3), 375–393 (2000)
3. Braak, H., Braak, E.: Neuropathological stageing of alzheimer-related changes. Acta neuropathologica **82**(4), 239–259 (1991)
4. Chen, M., Wei, Z., Huang, Z., Ding, B., Li, Y.: Simple and deep graph convolutional networks. In: ICML. Proceedings of Machine Learning Research, vol. 119, pp. 1725–1735. PMLR (2020)
5. Dan, T., Dere, M., Kim, W.H., Kim, M., Wu, G.: Tauflownet: Revealing latent propagation mechanism of tau aggregates using deep neural transport equations. Medical Image Analysis **95**, 103210 (2024)
6. Dan, T., Ding, J., Wei, Z., Kovalsky, S., Kim, M., Kim, W.H., Wu, G.: Re-think and re-design graph neural networks in spaces of continuous graph diffusion functionals. In: Advances in Neural Information Processing Systems. vol. 36, pp. 59375–59387 (2023)
7. Dan, T., Kim, M., Kim, W.H., Wu, G.: Tauflownet: Uncovering propagation mechanism of tau aggregates by neural transport equation. In: International Conference on Medical Image Computing and Computer-Assisted Intervention. pp. 77–86. Springer (2023)
8. Frost, B., Jacks, R.L., Diamond, M.I.: Propagation of tau misfolding from the outside to the inside of a cell. Journal of Biological Chemistry **284**(19), 12845–12852 (2009)

9. Grundke-Iqbal, I., Iqbal, K., Quinlan, M., Tung, Y.C., Zaidi, M.S., Wisniewski, H.M.: Microtubule-associated protein tau. a component of alzheimer paired helical filaments. Journal of Biological Chemistry **261**(13), 6084–6089 (1986)
10. LaMontagne, P.J., Benzinger, T.L., Morris, J.C., Keefe, S., Hornbeck, R., Xiong, C., Grant, E., Hassenstab, J., Moulder, K., Vlassenko, A.G., et al.: Oasis-3: longitudinal neuroimaging, clinical, and cognitive dataset for normal aging and alzheimer disease. MedRxiv pp. 2019–12 (2019)
11. Li, W., Yang, D., Yan, C., Chen, M., Li, Q., Zhu, W., Wu, G., Initiative, A.D.N., et al.: Characterizing network selectiveness to the dynamic spreading of neuropathological events in alzheimer's disease. Journal of Alzheimer's Disease **86**(4), 1805–1816 (2022)
12. Nelson, P.T., Alafuzoff, I., Bigio, E.H., Bouras, C., Braak, H., Cairns, N.J., Castellani, R.J., Crain, B.J., Davies, P., Tredici, K.D., et al.: Correlation of alzheimer disease neuropathologic changes with cognitive status: a review of the literature. Journal of Neuropathology & Experimental Neurology **71**(5), 362–381 (2012)
13. Otto, F.: The geometry of dissipative evolution equations: the porous medium equation (2001)
14. Raj, A., Kuceyeski, A., Weiner, M.: A network diffusion model of disease progression in dementia. Neuron **73**(6), 1204–1215 (2012)
15. Raj, A., LoCastro, E., Kuceyeski, A., Tosun, D., Relkin, N., Weiner, M.: Network diffusion model of progression predicts longitudinal patterns of atrophy and metabolism in alzheimer's disease. Cell Reports **10**(3), 359–369 (2015)
16. Sepulcre, J., Grothe, M.J., d'Oleire Uquillas, F., Ortiz-Terán, L., Diez, I., Yang, H.S., Jacobs, H.I., Hanseeuw, B.J., Li, Q., El-Fakhri, G., et al.: Neurogenetic contributions to amyloid beta and tau spreading in the human cortex. Nature medicine **24**(12), 1910–1918 (2018)
17. Velickovic, P., Cucurull, G., Casanova, A., Romero, A., Li, P., Bengio, Y.: Graph attention networks (2017)
18. Vogel, J.W., Iturria-Medina, Y., Strandberg, O.T., Smith, R., Levitis, E., Evans, A.C., Hansson, O.: Spread of pathological tau proteins through communicating neurons in human alzheimer's disease. Nature communications **11**(1), 2612 (2020)
19. Weiner, M.W., Veitch, D.P., Aisen, P.S., Beckett, L.A., Cairns, N.J., Cedarbaum, J., Donohue, M.C., Green, R.C., Harvey, D., Jack Jr, C.R., et al.: Impact of the alzheimer's disease neuroimaging initiative, 2004 to 2014. Alzheimer's & Dementia **11**(7), 865–884 (2015)
20. Wu, F., Jing, X., Wei, P., Lan, C., Ji, Y., Jiang, G., Huang, Q.: Semi-supervised multi-view graph convolutional networks with application to webpage classification. Inf. Sci. **591**, 142–154 (2022)
21. Wu, J.W., Hussaini, S.A., Bastille, I.M., Rodriguez, G.A., Mrejeru, A., Rilett, K., Sanders, D.W., Cook, C., Fu, H., Boonen, R.A., et al.: Neuronal activity enhances tau propagation and tau pathology in vivo. Nature neuroscience **19**(8), 1085–1092 (2016)
22. Zhang, J., Yang, D., He, W., Wu, G., Chen, M.: A network-guided reaction-diffusion model of at [n] biomarkers in alzheimer's disease. In: 2020 IEEE 20th International Conference on Bioinformatics and Bioengineering (BIBE). pp. 222–229. IEEE (2020)